# Sorption by solids with bidisperse pore structures

E. RUCKENSTEIN*, A. S. VAIDYANATHAN and G. R. YOUNGQUIST

Clarkson College of Technology, Potsdam, New York 13676, U.S.A.

**Abstract** — A bidisperse model for transient diffusion in porous systems consisting of small spherical particles is presented. Such a model describes sorption in pelletized particles and in some types of molecular sieves and ion exchange resins.

Experimental sorption rates in ion exchange resins obtained by the authors and those available in the literature are interpreted by means of the proposed theoretical equation.

A VARIETY of processes exist where diffusion in porous solids is of interest. Important among these are heterogeneous catalytic reactions, adsorption and ion exchange. Porous catalysts, adsorbents and ion exchangers contain irregular networks of pores of various sizes and shapes. The description of transport processes in such solids is inherently difficult owing to the complex and largely unknown nature of the pore network and because, depending on the dimensions of pores, the mechanisms of mass transport may be due to bulk diffusion, Knudsen diffusion, and surface diffusion. As a result, most models for diffusion in porous solids are approximate. Many of these have been reviewed elsewhere [1, 2].

The type of porous solid which is of particular interest here has a bidisperse pore size distribution. Such solids may be obtained in a variety of ways. When finely divided powder is tabletted, the resulting large particles generally have relatively large pores (macropores) consisting of spaces between the powder particles and small pores (micropores) from the powder particles themselves. Catalysts or adsorbents made by pelletizing an active powder (synthetic zeolites, for example) show the same result as do macroreticular ion exchange resins. Kun and Kunin[3] indicate that the ion exchange resins are agglomerates of randomly packed microspheres

with a continuous non-gel pore structure. Since the macropore diffusivity generally may be quite different in magnitude from the micropore diffusivity the particular structure of this type of porous solid may have a considerable effect on the rates at which diffusion processes occur. Wakao and Smith[4] have proposed a "random pore" model to describe diffusion in such solids, and Frisch[5] has considered diffusion limited reactions catalyzed by polymeric macroreticular ion exchange resins in which both macropore diffusion and matrix diffusion in the polymer are taken into account. Ruckenstein[6] has treated the effectiveness of diluted porous catalysts consisting of small spherical particles of active porous solid imbedded in a porous inactive solid. In the above mentioned references only the steady-state diffusion in a bidisperse medium has been treated.

In many cases where sorption by solids of gases, liquids or vapors occurs, the unsteady intraparticle diffusion is rate limiting. This is also true for ion exchange. Rate data have, for the most part, been analyzed using time dependent diffusion equations which largely ignore the structural details of the solid and their effects on the sorption rate. For example, when the concentration at the external surface is held constant, the rate of uptake by a spherical sorbent particle has been given by [7, 8]

---

$$\frac{M_t}{M_\infty} = 1 - \frac{6}{\pi^2} \sum_{n=1}^{\infty} \frac{1}{n^2} \exp\left[-\frac{n^2\pi^2 \mathscr{D} t}{R_a^2}\right] \quad (1)$$

where $\mathscr{D}$ is an effective intraparticle diffusivity. This type of rate model is appropriate when solid diffusion or diffusion in pores of uniform size is involved. However, in solids with bidisperse pore size distributions, diffusion and sorption occur simultaneously in both macropores and micropores and these competing effects must be considered. These effects have been observed experimentally on several occasions. Roberts and York[9] have reported rate data for sorption of liquid normal paraffins on Linde 5A molecular sieves which indicate that both macropore and micropore diffusion are important. These authors used an additive series resistance model to account for macropore–micropore effects. Similarly, Antonson and Dranoff[10] have shown that both macropore diffusion and micropore diffusion are important for the fixed bed sorption of ethane, also by Linde 5A molecular sieves. Sorption of sulfur dioxide by a polymeric macroreticular ion exchange resin was observed by Layton and Youngquist[11] to occur in two stages, a rapid initial stage attributed to adsorption of $SO_2$ in the macropores of the resin, followed by a very slow second stage due to penetration of the polymer matrix. Rate data for the initial uptake was analyzed by assuming the rate of matrix penetration to be negligible during this period. During the slow approach to equilibrium, adsorption in the macropores was assumed to be at equilibrium. Equation (1) was shown to apply to each stage, successively, in the first considering diffusion in the large pores of the macrospherical resin particle and in the second solid diffusion in microspherical polymer beads which make up the particle.

Although experimental evidence indicates that there are a number of systems for which both macropore diffusion and micropore diffusion are important during transient sorption, no model which clearly shows the influence of these effects has yet been developed. In the present study, an analysis of transient sorption in which the competing effects of macropore diffusion and micropore diffusion are considered is presented. The sorbent is exposed to an infinite source of sorbate such that the concentration at the surface of the sorbate particle remains constant and the uptake to equilibrium is observed. This corresponds, for example, to the experimental method frequently employed to study the rate of adsorption of gases or vapors on solids. Diffusion limited sorption is considered to occur both in the macropores and in the micropores of the bidisperse solid. A sorption rate model is developed which considers a spherical macroporous sorbent particle to be an assembly of small microporous spheres. The sorbate diffuses into macropores and adsorbs on the macropore walls concurrent with diffusion and sorption in the micropores. The sorption process is assumed to be isothermal and linear isotherms are taken to apply.

*Development of the model*

Consider a spherical macroporous particle which consists of small spherical microporous particles of uniform size and shown schematically in Fig. 1. The radius of the microspheres is much less than that of the macrosphere. The particle is initially at equilibrium with the surrounding fluid. At time zero, a stepchange in the concentration of the sorbate external of the particle is made. The sorbate diffuses into the macropores, adsorbs on the macropore walls, and also diffuses into the micropores and is sorbed there.

For the macroporous structure, one may write

$$\frac{D_a \epsilon_a}{r_a^2} \frac{\partial}{\partial r_a}\left[r_a^2 \frac{\partial C_a}{\partial r_a}\right] = \epsilon_a \frac{\partial C_a}{\partial t} + S_a \frac{\partial C_{sa}}{\partial t}$$

$$+ n4\pi R_i^2 \epsilon_i D_i \left(\frac{\partial C_i}{\partial r_i}\right)_{r_i = R_i} \quad (2)$$

where the first term is due to the variation of diffusional flux in the macropore, the second and third to accumulation in the macropore volume and on the macropore surface respectively and the fourth to the diffusional flux at the surface of the microspheres. The concentration
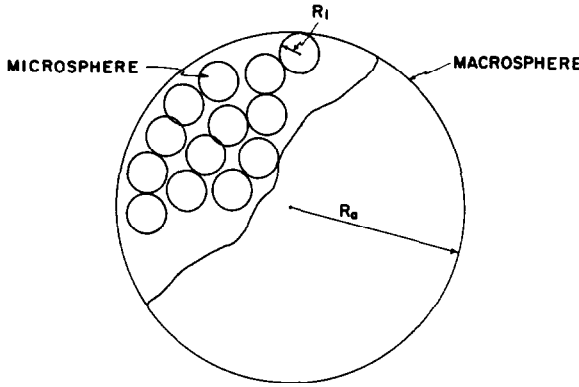
Fig. 1. Schematic diagram of a sorbent particle.

field inside the microsphere satisfies the equation:

$$D_i \frac{\epsilon_i}{r_i^2} \frac{\partial}{\partial r_i}\left[r_i^2 \frac{\partial C_i}{\partial r_i}\right] = \epsilon_i \frac{\partial C_i}{\partial t} + S_i \frac{\partial C_{si}}{\partial t}. \quad (3)$$

Assuming linear isotherms and equilibrium between fluid and sorbed phases in the pores,

$$C_{s_a} = H_a C_a$$
$$C_{s_i} = H_i C_i.$$

Equations (2) and (3) may be written

$$\frac{D_a}{r_a^2} \frac{\partial}{\partial r_a}\left[r_a^2 \frac{\partial C_a}{\partial r_a}\right] = \left[1 + \frac{H_a S_a}{\epsilon_a}\right]\frac{\partial C_a}{\partial t}$$

$$+ \delta D_i \left(\frac{\partial C_{0i}}{\partial r_i}\right)_{r_i = R_i} \quad (4)$$

$$\frac{D_i}{r_i^2} \frac{\partial}{\partial r_i}\left[r_i^2 \frac{\partial C_i}{\partial r_i}\right] = \left[1 + \frac{S_i H_i}{\epsilon_i}\right]\frac{\partial C_i}{\partial t}. \quad (5)$$

The initial and boundary conditions are:

$$C_a(0, r_a) = C_{a_0} = C_{i_0} \quad C_i(0, r_i) = C_{i_0} = C_{a_0}$$
$$C_a(t, R_a) = C_{a_\infty} = C_{i_\infty} \quad C_i(t, R_i) = C_a(t, r_a)$$

$$(6)$$

$$\frac{\partial C_a}{\partial r_a}(t, 0) = 0 \quad \frac{\partial C_i}{\partial r_i}(t, 0) = 0.$$

Defining the dimensionless variables

$$\theta_a = \frac{C_a - C_{a_0}}{C_{a_\infty} - C_{a_0}} \quad \theta_i = \frac{C_i - C_{i_0}}{C_{i_\infty} - C_{i_0}}$$

$$\eta = \frac{r_a}{R_a} \quad \gamma = \frac{r_i}{R_i}$$

$$\tau = \frac{D_a t}{\left(1 + \dfrac{S_a H_a}{\epsilon_a}\right) R_a^2}$$

and the parameters

$$\alpha = \frac{R_a^2 D_i \left(1 + \dfrac{S_a H_a}{\epsilon_a}\right)}{R_i^2 D_a \left(1 + \dfrac{S_i H_i}{\epsilon_i}\right)} = \frac{\mathscr{D}_i R_a^2}{\mathscr{D}_a R_i^2}$$

$$\beta = \frac{\delta D_i R_a^2}{R_i D_a} = \frac{3(1 - \epsilon_a)\epsilon_i}{\epsilon_a} \frac{R_a^2 D_i}{R_i^2 D_a}$$

Equations (4–6) become

$$\frac{1}{\eta^2} \frac{\partial}{\partial \eta}\left[\eta^2 \frac{\partial \theta_a}{\partial \eta}\right] = \frac{\partial \theta_a}{\partial \tau} + \beta\left(\frac{\partial \theta_i}{\partial \gamma}\right)_{\gamma=1} \quad (7)$$

$$\frac{\alpha}{\gamma^2} \frac{\partial}{\partial \gamma}\left[\gamma^2 \frac{\partial \theta_i}{\partial \gamma}\right] = \frac{\partial \theta_i}{\partial \tau} \quad (8)$$

$$\theta_a(0, \eta) = 0 \quad \theta_i(0, \gamma) = 0$$

$$\theta_a(\tau, 1) = 1 \quad \theta_i(\tau, 1) = \theta_a(\tau, \eta) \quad (9)$$

$$\frac{\partial \theta_a}{\partial \eta}(\tau, 0) = 0 \quad \frac{\partial \theta_i}{\partial \gamma}(\tau, 0) = 0. \quad (10)$$

These equations may be solved for $\theta_a$ with the result, (see Appendix),

$$\theta_a = 1 + \frac{4\pi}{\eta\beta} \sum_{k=1}^{\infty} \sum_{q=1}^{\infty}$$

$$\frac{(-1)^k k \sin(k\pi\eta) \exp[-\alpha\xi_{qk}^2 \tau]}{\xi_{qk}^2 \left[\dfrac{\alpha}{\beta} + 1 + \cot^2 \xi_{qk} - \left(1 - \dfrac{k^2\pi^2}{\beta}\right)\dfrac{1}{\xi_{qk}^2}\right]} \quad (11)$$

where $\xi_{qk}$ are the roots of the transcendental

equation

$$\beta(1 - \xi_{qk} \cot \xi_{qk}) + \alpha \xi_{qk}^2 = k^2\pi^2;$$

$$k = 1, 2, 3, \ldots, \infty. \quad (12)$$

The uptake is evaluated by determining the amount of sorbate which has entered the particle after changing the external concentration. That is,

$$M_t = \int_0^t D_a \epsilon_a 4\pi R_a^2 \left(\frac{\partial C_a}{\partial r_a}\right)_{r_a = R_a} dt. \quad (13)$$

At equilibrium,

$$M_\infty = \int_0^\infty D_a \epsilon_a 4\pi R_a^2 \left(\frac{\partial C_a}{\partial r_a}\right)_{r_a = R_a} dt. \quad (14)$$

From (11), (13) and (14) the fractional uptake is given by

$$\frac{M_t}{M_\infty} = \frac{\int_0^\tau \left(\frac{\partial \theta_a}{\partial \eta}\right)_{\eta = 1} d\tau}{\int_0^\infty \left(\frac{\partial \theta_a}{\partial \eta}\right)\bigg|_{\eta = 1} d\tau} =$$

$$\frac{\sum_{k=1}^\infty \sum_{q=1}^\infty \dfrac{k^2[1 - \exp(-\alpha \xi_{qk}^2 \tau)]}{\xi_{qk}^4 \left[\dfrac{\alpha}{\beta} + 1 + \cot^2 \xi_{qk} - \left(1 - \dfrac{k^2\pi^2}{\beta}\right)\dfrac{1}{\xi_{qk}^2}\right]}}{\sum_{k=1}^\infty \sum_{q=1}^\infty \dfrac{k^2}{\xi_{qk}^4 \left[\dfrac{\alpha}{\beta} + 1 + \cot^2 \xi_{qk} - \left(1 - \dfrac{k^2\pi^2}{\beta}\right)\dfrac{1}{\xi_{qk}^2}\right]}}. \quad (15)$$

## RESULTS AND DISCUSSION

As is evident from Eq. (15), the fractional uptake depends on the parameters $\alpha$ and $\beta$. The parameters $\alpha$ and $\beta$ have simple physical meanings. The parameter $\alpha$ may be written as

$$\alpha = \frac{\mathscr{D}_i R_a^2}{\mathscr{D}_a R_i^2} = \frac{(\mathscr{D}_i/R_i^2)}{(\mathscr{D}_a/R_a^2)} = \frac{t_m}{t_i}$$

where $t_m$ gives the order of magnitude of the time required for penetration of the macrosphere by diffusion and $t_i$, the time required

for penetration of the microsphere by diffusion. Therefore $\alpha$ represents the ratio of the time scales of the processes taking place in the macro and microspheres. Large values of $\alpha$ mean that the macropore diffusion process is rate limiting and very small values ($\alpha \ll 1$) indicate that micropore diffusion is rate controlling.

We may rewrite the parameter $\beta$ as

$$\beta = \frac{3(1 - \epsilon_a)\epsilon_i}{\epsilon_a} \alpha \frac{\left(1 + \dfrac{S_i H_i}{\epsilon_i}\right)}{\left(1 + \dfrac{S_a H_a}{\epsilon_a}\right)}.$$

Consequently $\beta/\alpha$ gives information concerning the ratio of the microsphere and macrosphere uptakes at equilibrium. (At equilibrium, their ratio is $1/3$ ($\beta/\alpha$)).

Thus, very small values of $\beta/\alpha$ indicate negligible microsphere uptake while for large values the macrosphere uptake is negligible. As stressed above the parameter $\alpha$ is a measure of the relative rates of uptake by the microspheres and the macrosphere. For values of $\alpha$ less than about $10^{-3}$, the uptake may be considered a two-stage sorption process. Diffusion and sorption in the macropores is much faster than in the micropores so that equilibrium is essentially achieved in the macropores before any measurable uptake by the micropores is observed. A first stage is observed during which only macropore sorption occurs, followed by a much slower second stage during which macropore sorption is at equilibrium and only micropore sorption occurs. For the first stage, the uptake is given by

$$\frac{M_a}{M_{a\infty}} = 1 - \frac{6}{\pi^2} \sum_{n=1}^\infty \frac{1}{n^2} \exp\left[-n^2\pi^2 \frac{\mathscr{D}_a t}{R_a^2}\right] \quad (16)$$

and for the second stage by

$$\frac{M_i}{M_{i\infty}} = 1 - \frac{6}{\pi^2} \sum_{n=1}^\infty \frac{1}{n^2} \exp\left[-n^2\pi^2 \frac{\mathscr{D}_i t}{R_i^2}\right]. \quad (17)$$

The total uptake at any time is the sum of the macrosphere uptake and the microsphere uptake.

Hence,

$$\frac{M_t}{M_\infty} = \frac{M_a + M_i}{M_{a\infty} + M_{i\infty}} = \frac{\dfrac{M_a}{M_{a\infty}} + \dfrac{M_i}{M_{i\infty}}\left(\dfrac{M_{i\infty}}{M_{a\infty}}\right)}{1 + \dfrac{M_\infty}{M_{a\infty}}}$$

$$= \frac{\dfrac{M_a}{M_{a\infty}} + \dfrac{1}{3}(\beta/\alpha)\dfrac{M_i}{M_{i\infty}}}{1 + \dfrac{1}{3}(\beta/\alpha)}. \qquad (18)$$

For times sufficiently large compared to $t_m$ but small compared to $t_i$ quasi-saturation is achieved in the macropore and one may consider that the microsphere surface concentration is practically constant (independent of time) and Eq. (17) may be used for the microsphere uptake. For such times, the macrosphere uptake is almost $M_{a\infty}$. Considering, however, the time dependence for $M_a$ given by (16) and ignoring any interaction between the two mechanisms, one obtains, by combining Eqs. (16–18):

macropores. As a result macropore diffusion is completely rate limiting and Eq. (15) reduces to

$$\frac{M_t}{M_\infty} = 1 - \frac{6}{\pi^2} \sum_{n=1}^{\infty} \frac{1}{n^2} \exp\left(\frac{-n^2\pi^2\tau}{1 + \frac{1}{3}\beta/\alpha}\right). \qquad (20)$$

Equation (20) may also be deduced simply by replacing the last term in Eq. (2) by $\frac{4}{3}\pi R_i^3 n \times$ $\left[\epsilon_i \dfrac{\partial C_i}{\partial t} + S_i \dfrac{\partial C_{s_i}}{\partial t}\right]$ and by assuming thermodynamic equilibrium between $C_i$ and $C_a$. Since the micropore uptake here is very rapid, the effect of the micropores is similar to that produced by adsorption in the macropores and reduces the apparent macropore diffusivity by the factor $1/[1 + (1/3) \times (\beta/\alpha)]$. Fig. 3 shows typical uptake curves.

The uptake for these two limiting cases may be determined readily by using the simpler Eqs. (19 and 20). For intermediate values of $\alpha$, however, Eq. (15) must be used. Figure 4 shows the uptake curves for $\alpha = 0.1$, 1 and 10, respectively, for various values of $\beta/\alpha$. As these

$$\frac{M_t}{M_\infty} = \frac{\left[1 - \dfrac{6}{\pi^2} \displaystyle\sum_{n=1}^{\infty} \dfrac{1}{n^2} \exp\left(-n^2\pi^2\tau\right)\right] + \dfrac{1}{3}(\beta/\alpha)\left[1 - \dfrac{6}{\pi^2} \displaystyle\sum_{n=1}^{\infty} \dfrac{1}{n^2} \exp\left(-n^2\pi^2\alpha\tau\right)\right]}{1 + \dfrac{1}{3}(\beta/\alpha)}. \qquad (19)$$

It should however be borne in mind that the above equation is valid only when $\left(\dfrac{6}{\pi^2} \displaystyle\sum_{n=1}^{\infty} \dfrac{1}{n^2} e^{-n^2\pi^2\tau}\right)$ $\ll 1$. The rigorous result is given by Eq. (15). Thus, a relatively rapid initial uptake due to the macropores occurs, reaching a quasi-equilibrium state at $M_t/M_\infty = 1/[1 + \frac{1}{3}(\beta/\alpha)]$, followed by a slow approach to equilibrium due to uptake by the micropores. Figure 2 indicates the rate behavior to be expected.

A second limiting case arises for large values of $\alpha$. If $\alpha$ is sufficiently large (greater than about 100), $t_i \ll t_m$, the concentration in the micro particles may be considered to be practically uniform throughout and in equilibrium with the corresponding local concentration in the

figures indicate, for fixed $\alpha$ the rate of approach to equilibrium decreases with increasing $\beta/\alpha$, reflecting the increasing fraction of the total sorption due to micropore sorption. Similarly, for fixed $\beta/\alpha$, the rate decreases with decreasing $\alpha$, reflecting a decrease in the rate of micropore sorption relative to the rate of macropore sorption.

The model presented suggests several characteristics of experimental sorption rate data which may be used to delineate the rate limiting features of the systems tested.

(1) *Macropore diffusion controls* ($\alpha > 10^2$)

The simplified Eq. (20) applies. The rate of approach to equilibrium is dependent on macrosphere size but independent of microsphere size.
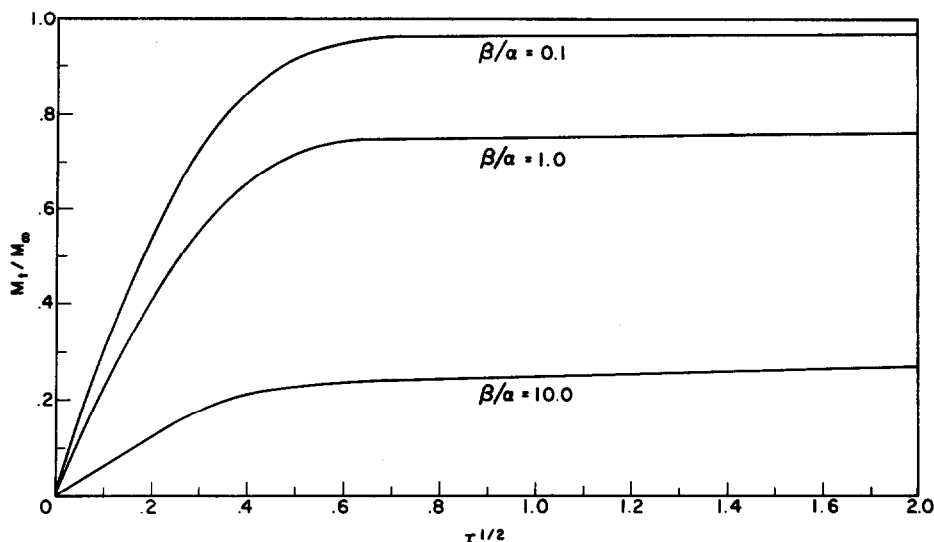
Fig. 2. Uptake curves for two stage sorption, $\alpha = 10^{-4}$.

**(2)** *Macropore diffusion much faster than micropore diffusion ($\alpha < 10^{-3}$)*

The simplified Eq. (19) applies. Sorption essentially occurs in two stages. A relatively rapid initial uptake due to macropore sorption (first stage) is followed by a slow approach to equilibrium due to micropore sorption (second stage). The rate of uptake during the first stage is dependent on macrosphere size but independent of microsphere size, while for the second stage the reverse is true.

**(3)** *Both macropore diffusion and micropore diffusion important ($10^{-3} < \alpha < 10^{2}$)*

Equation (15) applies. The rate behavior with respect to particle size is intermediate to (1)
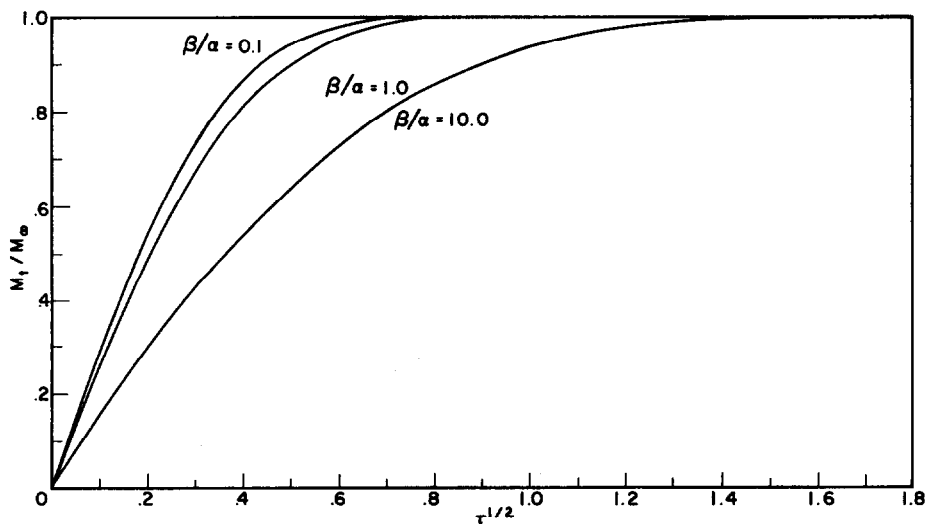


Fig. 3. Uptake curves with macropore diffusion control, $\alpha = 10^3$.
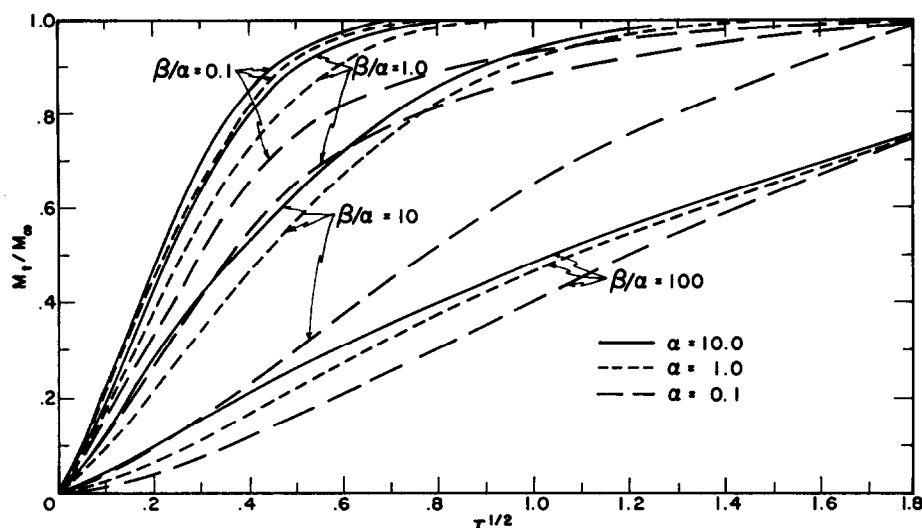
1310

Fig. 4. Effect of parameters on fractional uptake.

and (2) above. The rate of approach to equilibrium depends both on macrosphere size and on microsphere size.

Thus, an effective way to determine the relative importance of micropore and macropore diffusion is to conduct experiments where both the macrosphere and microsphere sizes are varied. To change the macrosphere size keeping the microsphere size constant is comparatively simple. However, considerable care must be exercised in the manufacture of macrospheres from microspheres of different sizes. If the macropore size distributions obtained from the use of different size microspheres are widely different, the diffusion and sorption properties

of the macropores may be sufficiently different to render comparative experiments meaningless.

It appears that a very wide range of values for the parameter $\alpha$ is possible. Table 1 gives some typical effective diffusivities and radii. Using these to calculate the extremes indicates that $\alpha$ may range from about $10^{-10}$ to $10^{+10}$, extending to both limiting cases. Thus, no a priori guidelines may be given for the rate limiting features of sorption systems of this type. However, in most cases sufficient diffusivity information will be available from prior experiments or may be predicted from theory so that $\alpha$ may be estimated to serve as a guide, in the analysis of experimental data. For example,

Table 1. Typical diffusivities and particle sizes

| | | |
|---|---|---|
| Effective macropore diffusivity, $\mathscr{D}_a$ | $10^{-2}$ cm²/sec | Diffusion of non adsorbing gases |
| | $10^{-5}$–$10^{-7}$ cm²/sec | Diffusion of liquids, diffusion with adsorption of gases |
| Effective micropore diffusivity, $\mathscr{D}_i$ | $10^{-3}$ cm²/sec | Diffusion of non-adsorbing gases |
| | $10^{-6}$–$10^{-10}$ cm²/sec | Diffusion and sorption of gases or liquids |
| | $10^{-6}$–$10^{-15}$ cm²/sec | Diffusion in polymers |
| Macrosphere radius, $R_a$ | $5 \times 10^{-2}$–$2 \times 10^{-1}$ cm | Adsorbent pellets or beads |
| Microsphere radius, $R_i$ | $10^{-4}$ cm–$10^{-5}$ cm | Powders |

the diffusivity and particle size data of Roberts and York[9] indicate that $\alpha$ is of the order of 0·1–1·0 which clearly indicates that both diffusion processes are important. Their rate data can not be analyzed using the present model, however, since in their case adsorption was irreversible and the model assumes linear equilibrium isotherms.

## EXPERIMENTAL

The MR ion exchange resin, obtained from Rohm and Haas Company, was dried, sieved and classified and about 30 mg of the required mesh sized sample was introduced in the Cahn electrobalance. The mesh size used in this particular study was that retained on No. 20 but passed through No. 16 Tyler standard. The whole assembly was evacuated to about 0·005 mm Hg and the sample heated [to 90°C for A–21; for A–15 it was 100°C] by means of heating tapes wound around the sample tube, until the recorder indicates no more weight loss. Heating is stopped, and the system is allowed to cool. The balance portion of the set up is isolated by means of a stop cock and the sample tube is kept immersed in a suitable constant temperature bath. The sorbate gas is filled in the rest of the equipment at the desired pressure. At time $t = 0$ the stop cock is opened and the sorbate gas is allowed to fill in the balance case instantaneously. Due to the rushing in of the gas the balance is disturbed and the recorder pen kicks back momentarily only to regain its initial

position within a very short time, at the most 30 sec. Sorption is allowed to proceed until equilibrium is achieved. Equilibrium is said to have been achieved, if over a period of 24 hr there is no further weight gain as indicated by the recorder. This took anywhere from few days to few weeks depending upon the sample, pressure increment, particle size, etc. The weight gain at any instant is divided by the equilibrium weight gain and this ratio is plotted against time. Once the equilibrium is reached the balance case is isolated once again by closing the stop cock, and the pressure in the rest of the equipment is adjusted to the required level. The sample is repeatedly exposed to the sorbate gas at different pressure levels "in steps". The isotherms for $SO_2$[11], water vapor[12], $CO_2$ and $NH_3$ are nonlinear. Yet, increasing the sorbate pressure "in steps", one could consider the isotherm to be "piece wise-linear" in the pressure interval used. Thus we come very close to the assumption of linear isotherm in our model.

In Fig. 6 are shown several rate data obtained by Layton and Youngquist[11] for $SO_2$, by Gupta [12] for water vapor and some of the data obtained by the authors for sorption of $CO_2$ and $NH_3$ on macroreticular polymeric ion exchange resins. For a more complete set of data Vaidyanathan's work[13] may be referred to. Properties of the resins used are given in Table 2. In each case, the resin was exposed to a step change in the sorbate concentration and the uptake to equilibrium was followed gravi-
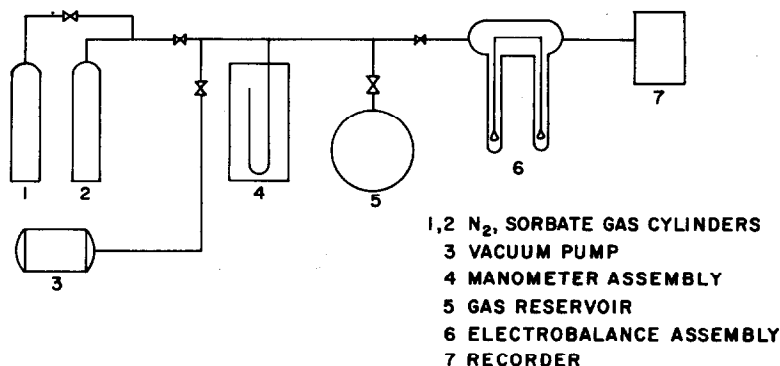


1,2 N₂, SORBATE GAS CYLINDERS
3 VACUUM PUMP
4 MANOMETER ASSEMBLY
5 GAS RESERVOIR
6 ELECTROBALANCE ASSEMBLY
7 RECORDER

Fig. 5. Experimental set up.

1312

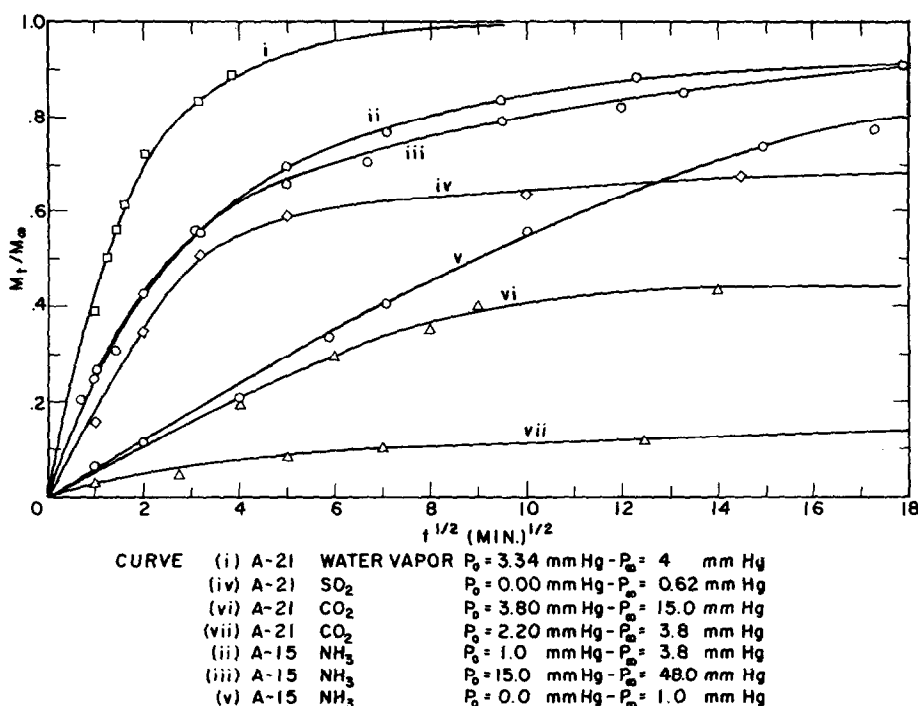| CURVE | (i) | A-21 | WATER VAPOR | $P_0 = 3.34$ mm Hg - $P_\infty$ = 4 mm Hg |
|---|---|---|---|---|
| | (iv) | A-21 | $SO_2$ | $P_0 = 0.00$ mm Hg - $P_\infty$ = 0.62 mm Hg |
| | (vi) | A-21 | $CO_2$ | $P_0 = 3.80$ mm Hg - $P_\infty$ = 15.0 mm Hg |
| | (vii) | A-21 | $CO_2$ | $P_0 = 2.20$ mm Hg - $P_\infty$ = 3.8 mm Hg |
| | (ii) | A-15 | $NH_3$ | $P_0 = 1.0$ mm Hg - $P_\infty$ = 3.8 mm Hg |
| | (iii) | A-15 | $NH_3$ | $P_0 = 15.0$ mm Hg - $P_\infty$ = 48.0 mm Hg |
| | (v) | A-15 | $NH_3$ | $P_0 = 0.0$ mm Hg - $P_\infty$ = 1.0 mm Hg |

Fig. 6. Experimental rate curves for sorption by macroreticular ion exchange resins.

metrically. A comparison of the experimental rate curves for the different sorbate–sorbent systems with theoretical rate curves gives some indication of possible rate characteristics of the system concerned.

The sorption of sulfur-dioxide on Amberlyst 21, a weak base resin, is characterized by two stage behavior consisting of a rapid initial uptake lasting a few minutes followed by a very slow weight gain. These rate curves resemble closely the rate curves shown in Fig. 2. This means, as indicated in the preceding discussions, that the value of the parameter $\alpha$ is of the order of $10^{-3}$ or less. In this case

a two stage process occurs, the relatively rapid initial uptake is probably due to macropore sorption without sorption in the microparticles, while the uptake during the very slow approach to equilibrium is due to the matrix penetration. Because the weight pick-up due to the initial uptake and the one due to the slow penetration are about the same, one may conclude that the value of the ratio $(\beta/3\alpha)$ would be of the order of magnitude of unity.

The carbon dioxide soprtion on the Amberlyst 21 system is also a two stage process. The shape of the experimental rate curve suggests, by comparison with the theoretical curves

Table 2. Ion exchange resin properties [3]

| Resin | Surface area $(m^2/g)$ | Macropore radius (Å) | Porosity $(cm^3/cm^3)$ | Macrosphere radius (mm) |
|---|---|---|---|---|
| A-15 | 54·8 | 60–300 | 0·357 | 0·59 |
| A-21 | 32·4 | 170–750 | 0·475 | 0·59 |

(Fig. 2), a predominantly matrix penetration dependent process as is marked by the small initial uptake, so that, unlike the $SO_2$-Amberlyst 21 system, $(\beta/\alpha)$ is large.

Sorption of water vapor on Amberlyst 21 shows no second stage sorption. This may indicate that the rate of macropore sorption and matrix penetration are comparable, or alternatively may indicate that one or the other is negligible. As discussed earlier, this point could be clarified by examining the effect of the particle size on the rate. Ammonia sorption on Amberlyst 15, a strong acid resin, shows a rate behavior that is somewhat intermediate to those for the other systems. It cannot be represented by the limiting Eqs. (19) or (20), but only by means of Eq. (15).

The evaluation of the parameters involves curve fitting the experimental data by trial and error. In Table 3 are given some approximate values of $\alpha$, $\beta$ and $\mathscr{D}_a/R_a^2$ (appearing in $\tau$)

minimum of 7 per cent (water vapor–A21 system) for the initial data points. The average deviation from the curve fitted value ranged from 4·5 per cent ($CO_2$–A21 system; curve vi) to 9 per cent ($CO_2$–A21 system; curve vii).

Of the four sorbates under consideration three, $SO_2$, $CO_2$ and water vapor, were sorbed by A21 and one, ammonia, was sorbed by A15. Curve (iv) in Figs. 6 and 7 represent sorption of $SO_2$ by a fresh resin which had no previous exposure to $SO_2$ and provided fresh surface in the macropore where $SO_2$ is readily sorbed. Hence a relatively high value for $M_a/M_i$ ($= 3\alpha/\beta$) is expected and the curve fit yields a value of 1·7. The curves (vii) and (vi) in Figs. 6 and 7 represent sorption of $CO_2$ by A21 at 3·8 mm Hg and 15 mm Hg respectively. In both cases, however, the sample had a previous history of exposures to $CO_2$; the sequence of exposures is $P_0 = 0·0$ mm Hg, $P_\infty = 0·2$ mm Hg; $P_0 = 0·2$ mm Hg, $P_\infty = 1·2$ mm Hg; $P_0 = 1·2$

Table 3. Sample values for the parameters (Fig. 7)

| System | Curve No. | $\alpha$ | $\beta$ | $(\mathscr{D}_a/R_a^2)$ (sec$^{-1}$) | $(\mathscr{D}_i/R_i)$ (sec$^{-1}$) | $\mathscr{D}_a$ (cm²/sec) | $\mathscr{D}_i$ (cm²/sec) | Error $\sigma$ |
|---|---|---|---|---|---|---|---|---|
| $SO_2$–A21 | (iv) | $1·0 \times 10^{-4}$ | $1·8 \times 10^{-4}$ | $2·0 \times 10^{-4}$ | $2·0 \times 10^{-8}$ | $7·0 \times 10^{-7}$ | $2·0 \times 10^{-18}$ | 0·00703 |
| $CO_2$–A21 | (vi) | $1·0 \times 10^{-4}$ | $4·0 \times 10^{-4}$ | $0·3 \times 10^{-4}$ | $0·3 \times 10^{-8}$ | $1·05 \times 10^{-7}$ | $3·0 \times 10^{-19}$ | 0·00187 |
| $CO_2$–A21 | (vii) | $1·0 \times 10^{-4}$ | $3·0 \times 10^{-3}$ | $1·0 \times 10^{-4}$ | $1·0 \times 10^{-8}$ | $3·5 \times 10^{-7}$ | $1·0 \times 10^{-18}$ | 0·00805 |
| $NH_3$–A21 | (v) | $1·0 \times 10^{-1}$ | $1·0 \times 10^{-1}$ | $3·12 \times 10^{-5}$ | $3·12 \times 10^{-6}$ | $9·36 \times 10^{-8}$ | $3·12 \times 10^{-16}$ | 0·00611 |
| $NH_3$–A21 | (ii) | $7·0 \times 10^{-2}$ | $6·0 \times 10^{-2}$ | $2·6 \times 10^{-5}$ | $1·8 \times 10^{-5}$ | $9·0 \times 10^{-7}$ | $1·8 \times 10^{-15}$ | 0·00300 |
| $NH_3$–A21 | (iii) | $8·0 \times 10^{-2}$ | $6·0 \times 10^{-2}$ | $1·67 \times 10^{-4}$ | $4·8 \times 10^{-5}$ | $5·0 \times 10^{-7}$ | $4·8 \times 10^{-15}$ | 0·00540 |
| Water vapor–A21 | (i) | $1·0 \times 10^2$ | $1·0 \times 10^2$ | $3·5 \times 10^{-4}$ | $3·5 \times 10^{-2}$ | $1·2 \times 10^{-6}$ | $3·5 \times 10^{-12}$ | 0·00195 |

obtained by curve fitting the experimental data (Fig. 7). The values obtained for the two effective diffusion coefficients are in the range of the data available in the literature (compare Tables 1 and 3) both for macropores and micropores. In calculating the micropore diffusion coefficient, the unknown microsphere radius has been assumed to be $10^{-5}$ cm. Error analyses were carried out for all the rate curves and the errors ($\sigma$) have been tabulated as shown in Table 3. The relative deviations between the observed and the curve fitted values were found to be maximum at small times and varied from a maximum of 20 per cent ($SO_2$–A21 system) to a

mm Hg, $P_\infty = 2·2$ mm Hg; $P_0 = 2·2$ mm Hg, $P_\infty = 3·8$ mm Hg (curve vii); $P_0 = 3·8$ mm Hg, $P_\infty = 15·0$ mm Hg (curve vi). In both the cases one would expect a major share of readily available macropore sites to be occupied by earlier exposures. Hence relatively low values of $M_{a\infty}/M_{i\infty}$ are expected and the curve fits yield values of 0·1 and 0·75 respectively. Water vapor A21 system represented by curve (i) in Figs. 6 and 7 had a history of previous exposures ($P_0 = 0·0$ mm Hg, $P_\infty = 0·53$ mm Hg; $P_0 = 0·53$ mm Hg, $P_\infty = 1·1$ mm Hg; $P_0 = 1·1$ mm Hg, $P_\infty = 1·63$ mm Hg; $P_0 = 1·63$ mm Hg, $P_\infty = 2·2$ mm Hg; $P_0 = 2·2$ mm Hg, $P_\infty = 2·77$ mm Hg;
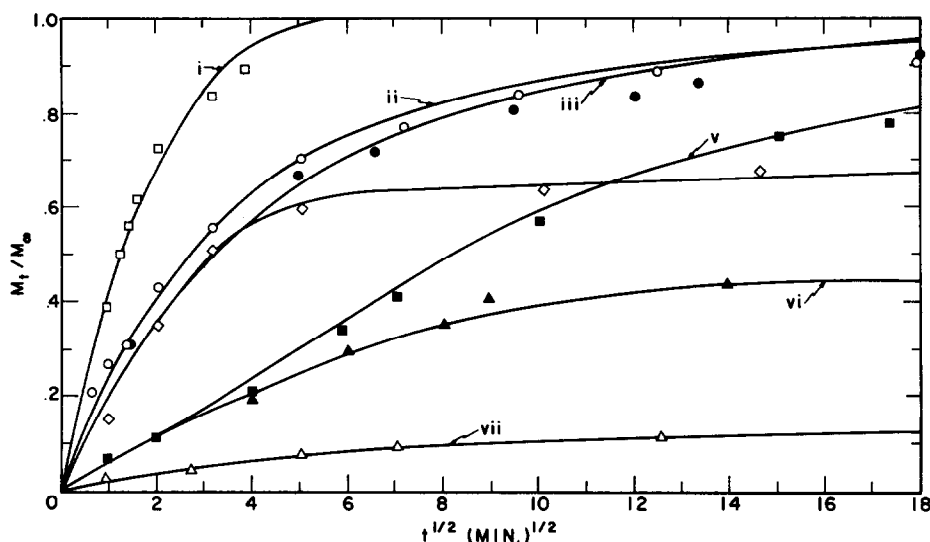
Fig. 7. Few curve fitted rate data (from Fig. 6).

$P_0 = 2 \cdot 77$ mm Hg, $P_\infty = 3 \cdot 34$ mm Hg; $P_0 = 3 \cdot 34$ mm Hg, $P_\infty = 4 \cdot 0$ mm Hg). One would expect a relatively high value for $M_{a_\infty}/M_{i_\infty}$ in this particular case; the curve fit yields a value of $3 \cdot 0$. Curves (v), (ii) and (iii) in Figs. 6 and 7 represent the rate data for sorption of $NH_3$ by A15 ion exchange resin at 1 mm Hg at $3 \cdot 8$ mm Hg and at 15 mm Hg respectively with the sequence of pressure jumps being $0 \cdot 0$ mm Hg to $1 \cdot 0$ mm Hg, $1 \cdot 0$ mm Hg to $3 \cdot 8$ mm Hg and $3 \cdot 8$ mm Hg to 15 mm Hg. The values of the ratio $M_{a_\infty}/M_{i_\infty}$ for these data were found by curve fitting to be $3 \cdot 0$, $3 \cdot 5$ and $4 \cdot 0$ respectively thereby indicating a higher sorption in the macropores.

## CONCLUSIONS

A model for transient sorption in solids having bidisperse pore structures which shows the influence of the competing effects of macropore and micropore diffusion has been developed. The model assumes that sorbent particles are spherical assemblies of porous microspheres and that diffusion and sorption occur both in the microspheres and in the macropores formed by the space between microspheres. Experimental methods useful for determining the relative importance of the two diffusion processes are suggested, and the model provides at least qualitative interpretation of previously reported experimental sorption data. A subsequent paper will treat fixed bed sorption.

## NOTATION

$C_a$ macropore fluid phase sorbate concentration, moles/cm$^3$

$C_{a_0}$ macropore fluid phase sorbate concentration at $t = 0$, moles/cm$^3$

$C_{a_\infty}$ macropore fluid phase sorbate concentration at equilibrium, moles/cm$^3$

$C_i$ micropore fluid phase sorbate concentration, moles/cm$^3$

$C_{i_0}$ micropore fluid phase sorbate concentration at $t = 0$, moles/cm$^3$

$C_{i_\infty}$ micropore fluid phase sorbate concentration at equilibrium, moles/cm$^3$

$C_{s_a}$ macropore adsorbed phase concentration, moles/cm$^2$

$C_{s_i}$ micropore adsorbed phase concentration, moles/cm$^2$

$D_a$ macropore diffusivity, cm$^2$/sec

$D_i$ micropore diffusivity, cm$^2$/sec

$\mathscr{D}$ effective diffusivity, cm²/sec

$\mathscr{D}_a$ $\dfrac{D_a}{1+\dfrac{H_a S_a}{\epsilon_a}}$, effective macropore diffusivity, cm²/sec

$\mathscr{D}_i$ $\dfrac{D_i}{1+\dfrac{H_i S_i}{\epsilon_i}}$, effective micropore diffusivity, cm²/sec

$H_a$ Henry's law constant for macropore adsorption, cm³/cm²

$H_i$ Henry's law constant for micropore adsorption, cm³/cm²

$M_a$ macropore uptake at time $t$

$M_{a_\infty}$ macropore uptake at equilibrium

$M_i$ micropore uptake at time $t$

$M_{i_\infty}$ micropore uptake at equilibrium

$M_t$ total uptake at time $t$

$M_\infty$ total uptake at equilibrium

$n$ number of microspheres per unit macrosphere volume

$P_0$ initial pressure in the system

$P_\infty$ operational pressure in the system

$r_a$ distance from macrosphere center, cm

$r_i$ distance from microsphere center, cm

$R_a$ macrosphere radius, cm

$R_i$ microsphere radius, cm

$S_a$ macropore surface area, cm²/cm³

$S_i$ micropore surface area, cm²/cm³

$t$ time, sec.

*Greek symbols*

$\alpha$ $\dfrac{\mathscr{D}_i R_a^2}{\mathscr{D}_a R_i^2}$, dimensionless rate parameter

$\beta$ $\dfrac{3(1-\epsilon_a)\epsilon_i}{\epsilon_a}\dfrac{R_a^2 D_i}{R_i^2 D_a}$, dimensionless parameter

$\beta/\alpha$ $\dfrac{3(1-\epsilon_a)\epsilon_i}{\epsilon_a}\dfrac{\left(1+\dfrac{H_i S_i}{\epsilon_i}\right)}{\left(1+\dfrac{H_a S_a}{\epsilon_a}\right)}=\dfrac{3M_{i_\infty}}{M_{a_\infty}}$, dimensionless equilibrium parameter

$\gamma$ $r_i/R_i$, dimensionless microsphere radial position

$\delta$ $\dfrac{3\epsilon_i}{R_i \epsilon_a}(1-\epsilon_a)$

$\epsilon_a$ macropore void fraction

$\epsilon_i$ micropore void fraction

$\eta$ $r_a/R_a$, dimensionless macrosphere radial position

$\theta_a$ $\dfrac{C_a - C_{a_0}}{C_{a_\infty} - C_{a_0}}$, dimensionless macropore concentration

$\theta_i$ $\dfrac{C_i - C_{i_0}}{C_{i_\infty} - C_{i_0}}$, dimensionless micropore concentration

$\tau$ $\dfrac{\mathscr{D}_a t}{R_a^2}$, dimensionless time

$\sigma$ error, $\sum\left[\dfrac{(M_t/M_\infty)_{\text{exptl.}} - (M_t/M_\infty)_{\text{predicted}}}{(M_t/M_\infty)_{\text{predicted}}}\right]^2$ / Number of exptl. points

## REFERENCES

[1] BARRER R. M., *Appl. Math. Res.* 1963 2 129.
[2] YOUNGQUIST G. R., *Ind. Engng Chem.* 1970 62 No. 8, 52.
[3] KUN K. and KUNIN R., *J. Polymer Sci.* 1967 C No. 16, 1457.
[4] WAKAO N., and SMITH J. M., *Chem. Engng Sci.* 1962 17 825.
[5] FRISCH N. W., *Chem. Engng Sci.* 1962 17 735.
[6] RUCKENSTEIN E., *A.I.Ch.E. Jl* 1970 16 151.
[7] CRANK J., *Mathematics of Diffusion.* Oxford, London, 1957.
[8] HELFFERICH F. G., *Ion Exchange.* McGraw-Hill, New York, 1962.
[9] ROBERTS P. V. and YORK R., *Ind. Engng Chem. Process Des. Develop.* 1967 6 516.
[10] ANTONSON C. R. and DRANOFF J. S., *Chem. Engng Prog. Symp.* 1969 Ser. No. 96, 65 27.
[11] LAYTON L. and YOUNGQUIST G. R., *Ind. Engng Chem. Process Des. Develop.* 1969 8 317.
[12] GUPTA V. K., M.S. Thesis in Chemical Engineering, Clarkson College of Technology 1969.
[13] VAIDYANATHAN A. S., Ph.D. Thesis in Chemical Engineering, Clarkson College of Technology, In press.

## APPENDIX

The diffusion equations are

$$\frac{1}{\eta^2}\frac{\partial}{\partial\eta}\eta^2\frac{\partial\theta_a}{\partial\eta}=\frac{\partial\theta_a}{\partial\tau}+\beta\left(\frac{\partial\theta_i}{\partial\gamma}\right)_{\gamma=1} \qquad \text{(i)}$$

and

$$\frac{\alpha}{\gamma}\frac{\partial}{\partial\gamma}\gamma^2\frac{\partial\theta_i}{\partial\gamma}=\frac{\partial\theta_i}{\partial\tau}. \qquad \text{(ii)}$$

Letting $\eta\theta_a = $ C and $\gamma\theta_i = $ N,

$$\frac{\partial^2 C}{\partial \eta^2} = \frac{\partial C}{\partial \tau} + \beta \eta \left[ \left( \frac{\partial N}{\partial \gamma} \right)_{\gamma=1} - (N)_{\gamma=1} \right] \qquad \text{(iii)}$$

$$\alpha \frac{\partial^2 N}{\partial \eta^2} = \frac{\partial N}{\partial \tau}. \qquad \text{(iv)}$$

Taking Laplace transform with respect to $\tau$ gives

$$\frac{\partial^2 \bar{C}}{\partial \eta^2} = s\bar{C} + \beta \eta \left[ \left( \frac{\partial \bar{N}}{\partial \gamma} \right)_{\gamma=1} - (\bar{N})_{\gamma=1} \right] \qquad \text{(v)}$$

and

$$\alpha \frac{\partial^2 \bar{N}}{\partial \gamma^2} = s\bar{N}. \qquad \text{(vi)}$$

Solving Eq. (vi) one obtains

$$\bar{N} = A \sinh \left[ (\sqrt{s/\alpha})\gamma \right] + B \cosh (\sqrt{s/\alpha}\gamma) \qquad \text{(vii)}$$

With the boundary conditions

$$\bar{N}(\gamma = 0) = 0$$

$$\bar{N}(\gamma = 0) = \frac{\bar{C}}{\eta}$$

(vii) becomes

$$\bar{N} = \frac{\bar{C}}{\eta} \frac{\sinh \left[ (\sqrt{s/\alpha})\gamma \right]}{\sinh \left[ (\sqrt{s/\alpha})\gamma \right]} \qquad \text{(viii)}$$

$$\left. \frac{\partial \bar{N}}{\partial \gamma} \right|_{\gamma=1} = \frac{\bar{C}}{\eta} (\coth \sqrt{s/\alpha}) \sqrt{s/\alpha}$$

$$\bar{N}|_{\gamma=1} = \frac{\bar{C}}{\eta}.$$

Substituting in Eq. (v),

$$\frac{\partial^2 \bar{C}}{\partial \eta^2} = s\bar{C} + \beta [(\sqrt{s/\alpha}) \coth (\sqrt{s/\alpha}) - 1]\bar{C} \qquad \text{(ix)}$$

which yields

$$\bar{C} = A \sinh (\eta [s + \beta((\sqrt{s/\alpha}) \coth (\sqrt{s/\alpha}) - 1)]^{1/2})$$
$$+ B \cosh (\eta [s + \beta((\sqrt{s/\alpha}) \coth (\sqrt{s/\alpha}) - 1)]^{1/2}). \qquad \text{(x)}$$

With the boundary conditions

$$\bar{C}(\eta = 0) = 0$$
$$\bar{C}(\eta = 1) = 1/s$$

one obtains

$$\bar{C} = \frac{1}{s} \frac{\sinh (\eta [s + \beta((\sqrt{s/\alpha}) \coth (\sqrt{s/\alpha}) - 1)]^{1/2})}{\sinh [s + \beta((\sqrt{s/\alpha}) \coth (\sqrt{s/\alpha}) - 1)]^{1/2}}. \qquad \text{(xi)}$$

Let $\xi = \sqrt{\dfrac{-s}{\alpha}}$ Eq. (xi) reduces to

$$\bar{C} = -\frac{1}{\alpha \xi^2} \frac{\sin (\eta[\alpha \xi^2 + \beta(1 - \xi \cot \xi)]^{1/2})}{\sin [\alpha \xi^2 + \beta(1 - \xi \cot \xi)]^{1/2}}. \qquad \text{(xii)}$$

Equation (xi) has a pole at $s = 0$ and an infinite number of poles defined by

$$\sin [\alpha \xi^2 + \beta(1 - \xi \cot \xi)]^{1/2} = 0$$

or

$$\alpha \xi^2 + \beta(1 - \xi \cot \xi) = k^2 \pi^2. \qquad \text{(xiii)}$$

Due to the transcendental nature of the above equation there will be an infinite number of roots for each value of $k$.

Using Heaviside Expansion theorem to invert (xii) gives

$$C = \eta \theta_a = \eta + \sum_{k=1}^{\infty} \sum_{q=1}^{\infty} \frac{(-1)^k \sin k\pi \eta\, e^{-\alpha \xi_{qk}^2 \tau}}{\xi_{qk}^2 \dfrac{d}{d\xi}\{\sin[\alpha \xi^2 + \beta(1 - \xi \cot \xi)]^{1/2}\}_{\xi = \xi_{qk}}} \qquad \text{(xiv)}$$

where $\xi_{qk}$ are the roots of Eq. (xiii)

$$\eta \theta_a = \eta + \frac{4\pi}{\beta} \sum_{k=1}^{\infty} \sum_{q=1}^{\infty} \frac{k(-1)^k \sin k\pi \eta\, e^{-\alpha \xi_{qk}^2 \tau}}{\xi_{qk}^2 \left[ \alpha/\beta + \left\{ 1 + \cot^2 \xi_{qk} - \left( 1 - \dfrac{k^2 \pi^2}{\beta} \right) \dfrac{1}{\xi_{qk}^2} \right\} \right]} \qquad \text{(xv)}$$

or

$$\theta_a = 1 + \frac{4\pi}{\beta \eta} \sum_{k=1}^{\infty} \sum_{q=1}^{\infty} \frac{k(-1)^k \sin k\pi \eta\, e^{-\alpha \xi_{qk}^2 \tau}}{\xi_{qk}^2 \left[ \alpha/\beta + \cot^2 \xi_{qk} - \left( 1 - \dfrac{k^2 \pi^2}{\beta} \right) \dfrac{1}{\xi_{qk}^2} \right]}. \qquad \text{(xvi)}$$

Taking the derivative with respect to $\eta$,

$$\left( \frac{\partial \theta_a}{\partial \eta} \right)_{\eta=1} = \frac{4\pi^2}{\beta} \sum_{k=1}^{\infty} \sum_{q=1}^{\infty} \frac{k^2\, e^{-\alpha \xi_{qk}^2 \tau}}{\xi_{qk}^2 \left[ \alpha/\beta + 1 + \cot^2 \xi_{qk} - \left( 1 - \dfrac{k^2 \pi^2}{\beta} \right) \dfrac{1}{\xi_{qk}^2} \right]}. \qquad \text{(xvii)}$$

Thus,

$$\frac{M_t}{M_\infty} = \frac{\displaystyle \int_0^\tau \left( \frac{\partial \theta_a}{\partial \eta} \right)_{\eta=1} d\tau}{\displaystyle \int_0^\infty \left( \frac{\partial \theta_a}{\partial \eta} \right)_{\eta=1} d\tau}$$

$$= \frac{\displaystyle \sum_{k=1}^{\infty} \sum_{q=1}^{\infty} \frac{k^2 [1 - \exp(-\alpha \xi_{qk}^2 \tau)]}{\xi_{qk}^4 \left[ \dfrac{\alpha}{\beta} + 1 + \cot^2 \xi_{qk} - \left( 1 - \dfrac{k^2 \pi^2}{\beta} \right) \dfrac{1}{\xi_{qk}^2} \right]}}{\displaystyle \sum_{k=1}^{\infty} \sum_{q=1}^{\infty} \frac{k^2}{\xi_{qk}^4 \left[ \dfrac{\alpha}{\beta} + 1 + \cot^2 \xi_{qk} - \left( 1 - \dfrac{k^2 \pi^2}{\beta} \right) \dfrac{1}{\xi_{qk}^2} \right]}}. \qquad \text{(xviii)}$$

**Résumé**—On présente un modèle à dispersion double pour la diffusion transitoire dans des systèmes poreux, consistant en de petites particules sphériques. Un tel modèle décrit la sorption dans des particules comprimées et dans quelques types de tamis moléculaires et de résines à échange d'ions.

Les vitesses expérimentales de sorption dans les résines à échange d'ions obtenues par les auteurs ainsi que celles décrites dans la littérature sont interprétées à l'aide de l'équation théorique proposée.

E. RUCKENSTEIN, A. S. VAIDYANATHAN and G. R. YOUNGQUIST

**Zusammenfassung** — Es wird ein bidisperses Modell für vorübergehende Diffusion in porösen Syste-men, bestehend aus kleinen, kugelförmigen Teilchen, dargelegt. Ein derartiges Modell beschreibt die Sorption in kugeligen Teilchen und in gewissen Arten von Molekularsieben und Ionenaustausch-harzen.

Die Autoren vergleichen die von ihnen erhaltenen Sorptionsraten in Ionenaustauschharzen mit den aus der Literatur erhältlichen auf Grund der vorgeschlagenen theoretischen Gleichung.